

# Numerical Simulation of Hydrodynamics and Residence Time in Alpine Lake with Three-Dimensional Model

Wen-Cheng Liu, Ming-Hsi Hsu and Wei-Bo Chen

## 1 Introduction

In aquatic environment such as shallow lakes, can stratify and destratify in a day, and may even remain persistently stratified over a couple of days. The entire water column in a shallow lake can behave as a diurnal mixed layer. The diurnal physical dynamics and the dynamics of phytoplankton [7], dissolved oxygen [1, 2], phosphorus [8], water color [12], methane [6], and other biogeochemical processes have been investigated.

Typhoon-induced inflow in Taiwan is an important factor to affect the mixing in the water column. Vertical mixing by turbulence in the mixed layer and circulation due to meteorological conditions have been numerically studied using one-dimensional mixed layer and two-dimensional, three-dimensional circulations models. Most of the existing numerical models are based on solving the shallow water equations, together with diffusion equations for the transport and dispersion of constituents and pollutants. Many two-dimensional models [3–5, 9] have been developed, but the deployment of two-dimensional models to simulate vertical

---

W.-C. Liu (✉) · M.-H. Hsu  
Department of Civil and Disaster Prevention Engineering,  
National United University, Miaoli 36003, Taiwan  
e-mail: weliu@nuu.edu.tw

W.-C. Liu  
Taiwan Typhoon and Flood Research Institute, National Applied Research Laboratories,  
Taipei 10093, Taiwan

M.-H. Hsu  
Department of Bioenvironmental Systems Engineering,  
National Taiwan University, Taipei 10617, Taiwan

W.-B. Chen  
National Science and Technology Center for Disaster Reduction, New Taipei City 23143,  
Taiwan

mixing, circulation, and wind-induced currents is not appropriate because the three-dimensional characteristics exist in the lakes. In recent years, a variety of three-dimensional models have been developed to simulate the hydrodynamics and wind-induced circulation, enabling to predict the substantial variation and reversal of the current along the bed induced by the wind action.

In the present study, a real-time three-dimensional hydrodynamic and hydro-thermal model is adopted to simulate water temperature and circulation in the stratified lake. Model simulation was validated against water level, current, time-series water temperature, and vertical profiles of water temperature in 2008. The validated model was then applied to investigate the wind-driven current and mean circulation in the Yuan-Yang Lake (YYL). The lake's residence time was also calculated and discussed using the validated model.

## 2 Description of Study Site

Yuan-Yang Lake (YYL) is in the northeastern region of Taiwan (24°35'N, 121°24'E) (Fig. 1a). YYL is a small (3.6 ha), shallow (4.5 m maximum depth) lake in a mountainous catchment 1,730 m above sea level. Figure 1b shows the bathymetry of YYL. The lake and surrounding catchment (374 ha) were designated as a long-term ecological study site by the Taiwan National Science Council in 1992 and joined the Global Lake Ecological Observatory Network (GLEON) in 2004. The steep watersheds are dominated by pristine Taiwan false cypress [*Chamaecyparis obtusa* Sieb. & Zucc. var. *formosana* (Hayata) Rehder] forest. YYL is slightly stained, with an average DOC concentration of 6.1 mg L<sup>-1</sup> and mean pH of 5.9. The average annual temperature is approximately 13 °C (monthly average ranges from -5 to 15 °C) and the annual precipitation is more than 4,000 mm. YYL is subject to three to seven typhoons in summer and autumn each year, during which more than 1,700 mm of precipitation may fall on the lake [11].

An instrumented buoy was deployed at the deepest spot in YYL (Fig. 1b) to record surface dissolved oxygen (DO), water temperature, and wind speed every 10 min. Surface DO concentrations were measured at 0.25 m depth by a sonde (600-XLM, YSI, Inc. Yellow Springs, OH, U.S.A.) fitted with a rapid-pulse oxygen-temperature electrode (YSI, model 6562). Water temperatures were measured through the water column at 0.5 m increments by a thermistor chain (Templine, Apprise Technologies, Inc. Duluth, MN, U.S.A.). Wind speed was measured 1 m above the lake by an anemometer (model 03001, R.M. Young, Traverse, MI, U.S.A.). Precipitation, air temperature, and downwelling photosynthetically active radiation (PAR) were measured at a land-based meteorological station approximately 1 km away from the lake. Variation in water level was measured using a submersible pressure transmitter (PS 9800(1), Instrumentation Northwest, Kirkland, WA, U.S.A.) deployed at the lake shore (Fig. 1b).

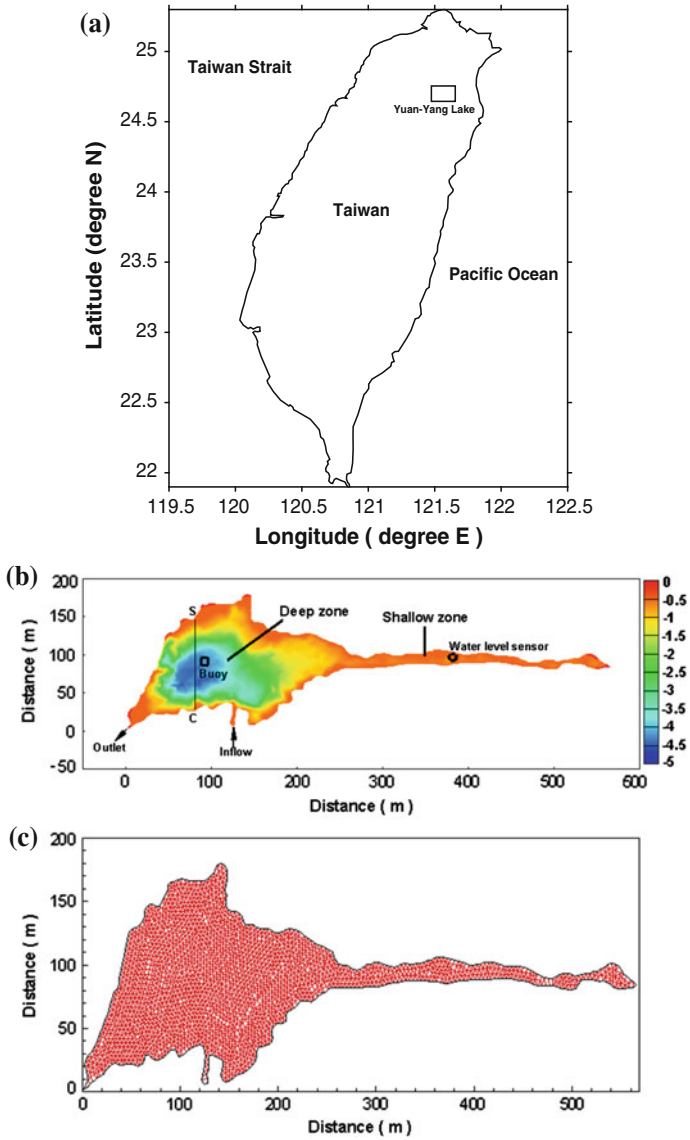


**Fig. 1** a Location of Yuan-Yang lake in Taiwan, b bathymetry, buoy, and water level locations, and c unstructured horizontal grid of Yuan-Yang Lake

### 3 Numerical Model

In this paper, a three-dimensional semi-implicit Eulerian–Lagrangian finite element model [17] was implemented to the YYL. SELFE solves the Reynolds-stress averaged Navier–Stokes equations consisting of conservation laws for mass, momentum, and temperature, under the hydrostatic and the Boussinesq approximations, to yield the free surface elevation, three-dimensional water velocity and water temperature.

$$\nabla \cdot \vec{u} + \frac{\partial w}{\partial z} = 0 \quad (1)$$

$$\frac{\partial \eta}{\partial t} + \nabla \cdot \int_{-h}^{\eta} \vec{u} dz = 0 \quad (2)$$

$$\begin{aligned} \frac{D\vec{u}}{Dt} &= \mathbb{F} - g\nabla\eta + \frac{\partial}{\partial z}(v\frac{\partial\vec{u}}{\partial z}) \\ \mathbb{F} &= -f\vec{k} \times \vec{u} + \alpha g\nabla\hat{\psi} - \frac{1}{\rho_0}\nabla P_A - \frac{g}{\rho_0}\int_z^{\eta}\nabla\rho d\zeta + \nabla \cdot (\mu\nabla\vec{u}) \end{aligned} \quad (3)$$

$$\frac{DT}{Dt} = \frac{\partial}{\partial z}(K_{sv}\frac{\partial T}{\partial z}) + \frac{\dot{Q}}{\rho_0 C_p} + F_h \quad (4)$$

$$\rho = \rho_0(p, T) \quad (5)$$

where  $(x, y)$ : horizontal Cartesian coordinates;  $z$ : vertical coordinate, positive upward;  $\nabla: (\frac{\partial}{\partial x}, \frac{\partial}{\partial y})$ ;  $t$ : time;  $\eta(x, y, t)$ : free surface elevation;  $h(x, y)$ : bathymetric depth;  $\vec{u}(x, y, z, t)$ : horizontal velocity, with Cartesian components  $(u, v)$ ;  $w$ : vertical velocity;  $f$ : Coriolis factor;  $g$ : acceleration of gravity;  $\hat{\psi}(\phi, \lambda)$ : earth tidal potential;  $\alpha$ : effective Earth elasticity factor;  $\rho(x, t)$ : water density; by default, reference value  $\rho_0$  is set as 1025 kg/m<sup>3</sup>;  $P_A(x, y, t)$ : atmospheric pressure at the free surface;  $p$ : pressure;  $T$ : water temperature;  $v$ : vertical eddy viscosity;  $\mu$ : horizontal eddy viscosity;  $K_{sv}$ : vertical eddy diffusivity for water temperature,  $F_h$ : horizontal diffusion for transport equation;  $\dot{Q}$ : rate of absorption of solar radiation; and  $C_p$ : specific heat of water.

SELFE model is based on a finite element scheme. Unlike most three-dimensional models, no mode splitting is allowed. Semi-implicit schemes are applied to all equations to enhance stability and to maximize efficiency. An Eulerian–Lagrangian method (ELM) is used to treat the advection, thus allowing large time step to be used without compromising stability. The entire domain is discretized in the horizontal and vertical directions. Unstructured triangular grids are used in the horizontal direction.

In the vertical, models based on terrain-following coordinates suffer, to some degree, from the hydrostatic inconsistencies. This follows from the fact that terrain-following coordinates do not conform to the geopotential, and the pressure gradient is evaluated as the difference between two large components that tend to cancel each other, thus being to large discretization errors. It can also be viewed as result of evaluating pressure at a grid point efficiently using extrapolation when steep bathymetric slopes are presented [16]. Many remedies have been used to prevent this, including evaluating the gradient in the Z-coordinate [16] or applying high-order schemes [14]. In the present model, the use of a hybrid coordinate system in the vertical effectively wards off the hydrostatic inconsistency because the Z-coordinates used in the deeper part of the vertical serves to “stabilize”, while S-coordinates used at the upper part of the water column.

SELFE uses the Generic Length Scale (GLS) turbulence closure of Umlauf and Burchard [15] which has the advantage of encompassing most of the 2.5-equation closure model. The detailed description of turbulence closure model, vertical boundary conditions for the momentum equation, the numerical solution methods, and numerical stability can be found in [17].

In this study, the bottom topography data in the YYL which were measured in August, 2007, were obtained from the Academia Sinica, Taiwan. The deepest depth within the study area is 4.5 m near the buoy station (Fig. 1b). The model mesh for the YYL consists of 4,148 polygons in horizontal direction (Fig. 1c). High solution grids which include the mesh size ranged from 3.2 to 6.6 m are used in the YYL. The terrain-following “pure S” layers were adopted in vertical direction and 20 evenly spaced S-levels were used. The “pure S” representation of SELFE was chosen to avoid the staircase representation of the bottom and surface, and thus loss of accuracy. For this model grid, a large time step ( $\Delta t = 120$  s) was used in simulations with no sign of numerical instability. It means that 263520 time steps for 1 year simulation. One year of simulation takes about 2.5 days on an Intel Core I5 PC.

## 4 Model Validation

The SELFE has been successfully applied to several estuaries and coastal oceans [10, 17], but little used to lakes. To ascertain the model accuracy for practical application, a large set of observational data is used to validate the model and to verify its capability to predict water surface elevation, residual current, and water temperature in this study.

### 4.1 Water Surface Elevation and Velocity

The model validation of water surface elevation was conducted with daily discharge at the inflow and outlet in the lake (shown in Fig. 1b). Figure 2a presents the

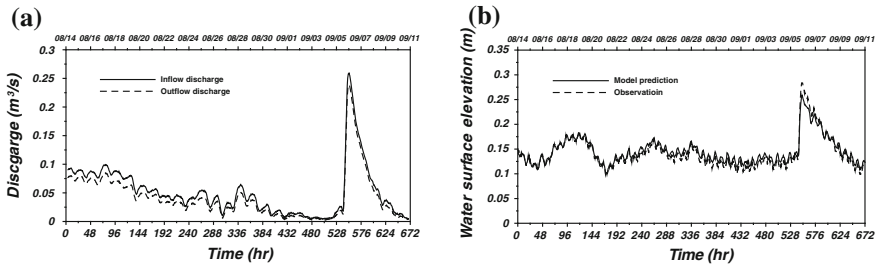


**Fig. 2** **a** Time-series inflow and outflow discharges and **b** Comparison of water surface elevation between model prediction and observation from August 14 to September 10, 2008

time-series inflow and outflow discharges. It reveals that the peak discharge occurred on September 6 due to the typhoon event. The observed water surface elevations in the YYL from August 14 to September 10, 2008 were used to compare with model predictions shown in Fig. 2b.

Good model performance is indicated by the calculated absolute mean error (AME) and root-mean-square error (RMSE) statistic values. AME is the average of the absolute values of differences between observed data and simulated values. RMSE basically specifies the overall difference in the sum of squares normalized to the number of observations. Both AME and RMSE provide an indication of the magnitude of the model’s prediction uncertainty for a type data point. RMSE is similar to a standard error of the mean for the model’s uncertainty. The AME and RMSE between computed and observed water surface elevation are 0.65 and 0.79 cm, respectively. It reveals that the simulated results mimic the observed water surface elevations.

Figure 3 presents the comparison of model simulated and measured velocity profiles at the buoy station on September 16, 2008. It shows that the return current occurred in the velocity profiles at *u* and *v* components. The simulated results closely match the measured velocity profiles and indicate that the model has the capability to predict the current patterns in the lake.

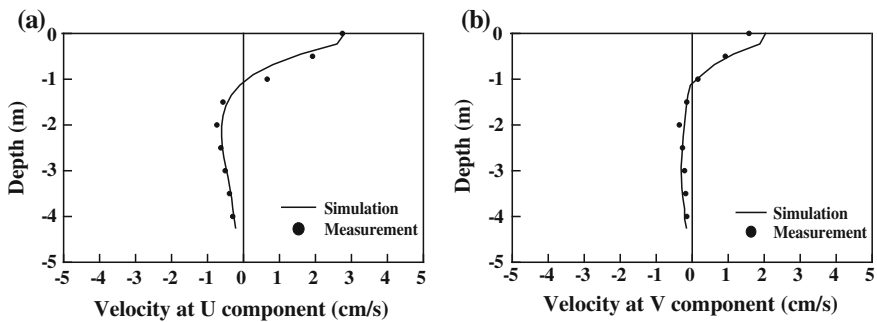


**Fig. 3** Comparison of model simulated and measured velocities on September 16, 2008 at the **a** *u* component, and **b** *v* component

### 4.2 Water Temperature

To validate the water temperature, the time-series data collected from July to September 2008 was used to compare with simulated results. Figure 4a presents the comparison of model predicted and measured water temperature at depths 0.25 and 3.5 m from July 6 to September 4, 2008. Two typhoon events hit Taiwan during July 16–18 and July 26–29 and resulted in well mixing conditions because the high precipitation and inflow occurred during these periods. The AME and RMSE between computed and observed water temperature at 0.25 m depth are 0.96 °C and 1.47 °C, respectively, while AME and RMSE at 2.0 m depth are 0.50 °C and 0.97 °C, respectively. Figure 4b–d illustrate the observed and calculated water temperature profiles at three time periods.

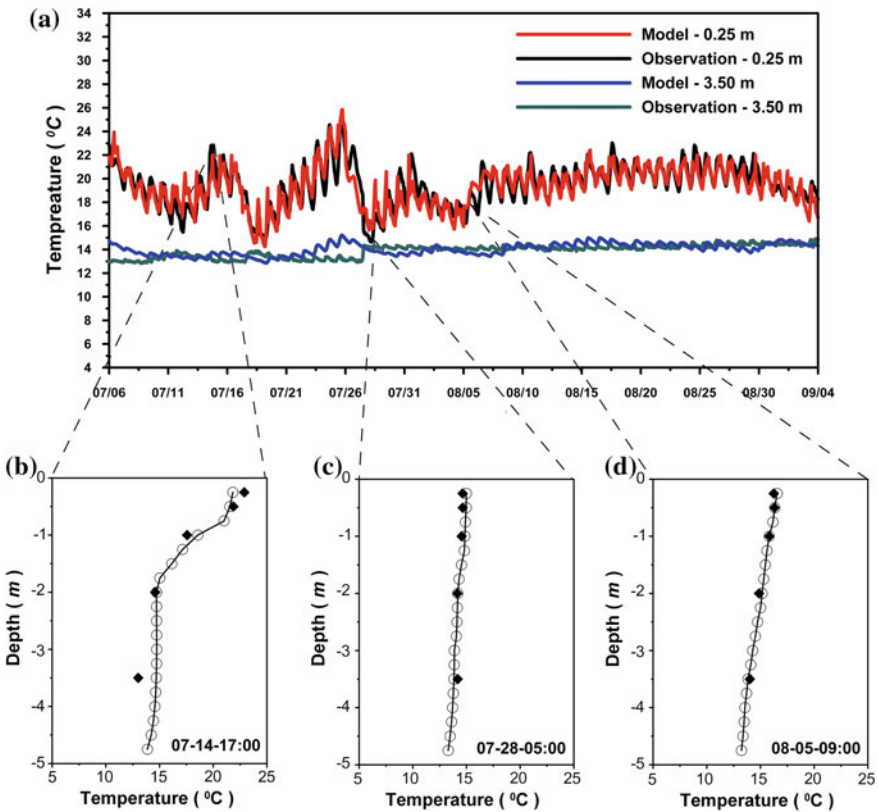


**Fig. 4** a The comparison of model predicted (*open circles line*) and measured (*diamond*) water temperature in the YYL from July to September 2008. Vertical temperature profile at different time spans **b** 17:00 July 14, **c** 5:00 July 28, and **d** 9:00 August 5

## 5 Mean Circulation and Residence Time

### 5.1 Mean Circulation

The mean circulation in the YYL is one of the important factors responsible for the transport and distribution of nutrients within the lake. In order to examine how the nutrients could be distributed in the YYL, the mean circulation of the model that runs for the period of May 1 to June 30, 2008 was yielded (Fig. 5). The large-scale patterns of the mean surface circulation produced by the model follows the general wind pattern over the area. The surface currents, in general flow toward the southwest direction and forms a clockwise rotation. The bottom currents are in opposite direction as surface currents due to return flows. The near-bottom currents are smaller than surface currents. The mean surface currents were between 1.1 and 3.6 cm/s. The mean surface temperature during this whole period was around 22 °C at the shallow area and 19 °C at the deep region. The mean temperature difference between the surface and bottom was around 5 °C in the deeper region. No remarkable cyclonic and anticyclonic circular gyres were found in the lake through the simulated mean currents.

### 5.2 Residence Time

The evaluation of the mean residence time of water in a lake is a problem of fundamental importance for theoretical and applied limnology. It can lead to the knowledge of the proportions and dynamics of the chemical substances dissolved in the water, or the rate at which the processes of concentration, dilution, and permanence of substances within the lake occur, with resulting implications for the water quality.

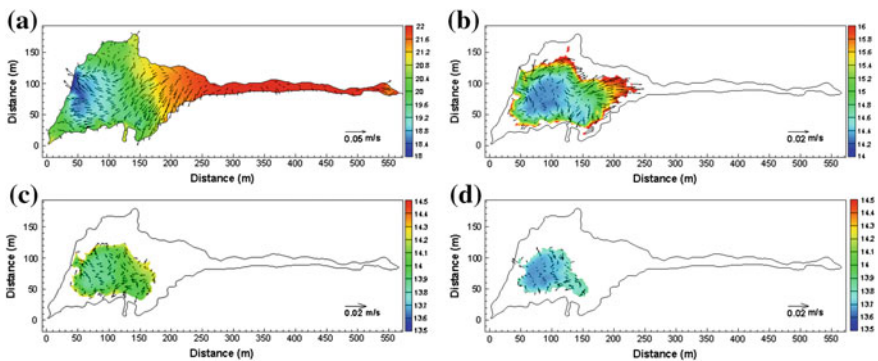


**Fig. 5** Mean circulation and average temperature during May and June 2008 at **a** surface **b** 1 m below surface, **c** 2 m below surface, and **d** 3 m below water surface



A first-order description of transport is expressed as “residence time” or “flushing time”, a measure of water mass retention within defined boundaries. Aquatic scientists often estimate retention time to compare to time scales of input or biogeochemical processes to calculate mass balances or understand dynamics of population and chemical properties [13].

The residence time is preferred in this study to investigate the possibility of physical transport mechanisms. The experiment was conducted with a certain amount of mass,  $m_0$ , of a conservative tracer injected at time  $t_0$  and at certain location. The time varying tracer mass,  $m(t)$ , remaining in the water body is then measured. The quantity  $m(t)$  is found from the spatial integration of the measured concentration field within the water body, and its decline over time reflects the net rate at which tracer leaves the water body. The rate of mass loss as a function of time  $r(t)$  provides residence time distribution,  $\varphi(t)$ ,

$$r(t) = \varphi(t) = -\frac{1}{m_0} \frac{dm}{dt} \tag{6}$$

Equation (1) represents the residence time distribution of unit,  $[T]^{-1}$ . The mean residence time, based on the first moment of  $r(t)$ , can be calculated as

$$T_r = \int_0^\infty r(t)t dt = -\frac{1}{m_0} \int_0^\infty t \left[ \frac{dm}{dt} \right] dt \tag{7}$$

where  $t$  is time and  $T_r$  is the mean residence time.

One issue remains in the application of Eq. (7) is the upper limit of the integration. Theoretically, the integration should be processed to the time when the residual mass reaches zero. In most circumstances, it may take infinitely long time. In this study, we adopt 1 % of residual mass which is designed to be the upper limit of the integration in Eq. (7).

The validated three-dimensional hydrodynamic and hydrothermal model was used to calculate the residence time in response to different inflow discharges with and without wind effects in the YYL. Tracer concentration of 10 was occupied in the lake and then the model was run with different discharges from inflow boundaries. To investigate the wind effects on the residence time, the model was forced with northeast wind, southwest wind, and without wind stress. The wind speed was specified with 1.4 m/s when wind stress was included.

Figure 6 plots the residence time versus the inflow discharge with and without wind effects. In all three scenario runs, data obtained from hydrodynamic and hydrothermal model simulations indicate that residence time reduce in response to inflows in a similar pattern. Least square regression analysis was conducted. Empirical best-fitting equations were obtained in forms of power law. The power law empirical equations fit well with the residence time resulted from the hydrodynamic and hydrothermal model simulations, with correlation  $R^2$  values above 0.97. Empirical regression equations of residence time ( $T_r$ ) versus inflows ( $Q$ ) are given below:

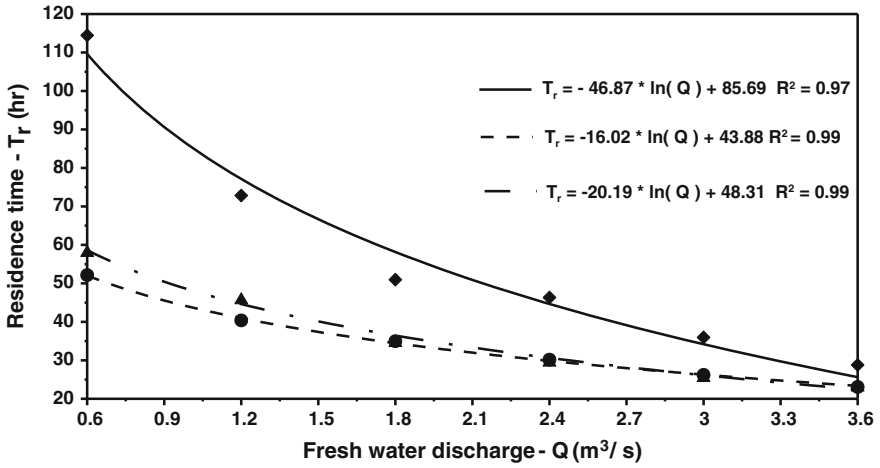


**Fig. 6** Residence time ( $T_r$ ) corresponding to the different discharges ( $Q$ ), which include without wind effect (solid line and diamonds), with northeast wind (dashed line and circles), and with southwest wind (dotted-dashed line and triangles)

(a) Without wind stress:

$$T_r = -46.87 \cdot \ln(Q) + 85.69, R^2 = 0.97 \quad (8)$$

(b) With northeast wind effect:

$$T_r = -16.02 \cdot \ln(Q) + 43.88, R^2 = 0.99 \quad (9)$$

(c) With southwest wind effect:

$$T_r = -20.19 \cdot \ln(Q) + 48.31, R^2 = 0.99 \quad (10)$$

where  $R^2$  is coefficient of determination.

The simulated results reveal that the residence time without wind stress is higher than that with wind stress, indicating that wind plays a significant role in mixing in the lake. The residence time with southwest wind is slightly higher than that with northeast wind. A shorter residence time is beneficial to pollutant removal.

When the inflow is  $0.6 \text{ m}^3/\text{s}$ , the distribution of tracer concentration at cross-section C–S (see Fig. 1b) at 48th h with and without wind effects is presented in Fig. 7. It reveals that the obvious stratification in trace concentration and the concentration at the bottom layer is higher than that at the surface layer. The bottom concentration without wind effect is higher than that with wind effect. The bottom concentration with southwest wind is also higher than that with northeast wind. It means that the residence time is higher without wind effect because it takes longer time to reach 1 % of residual mass presented in Eq. (7).

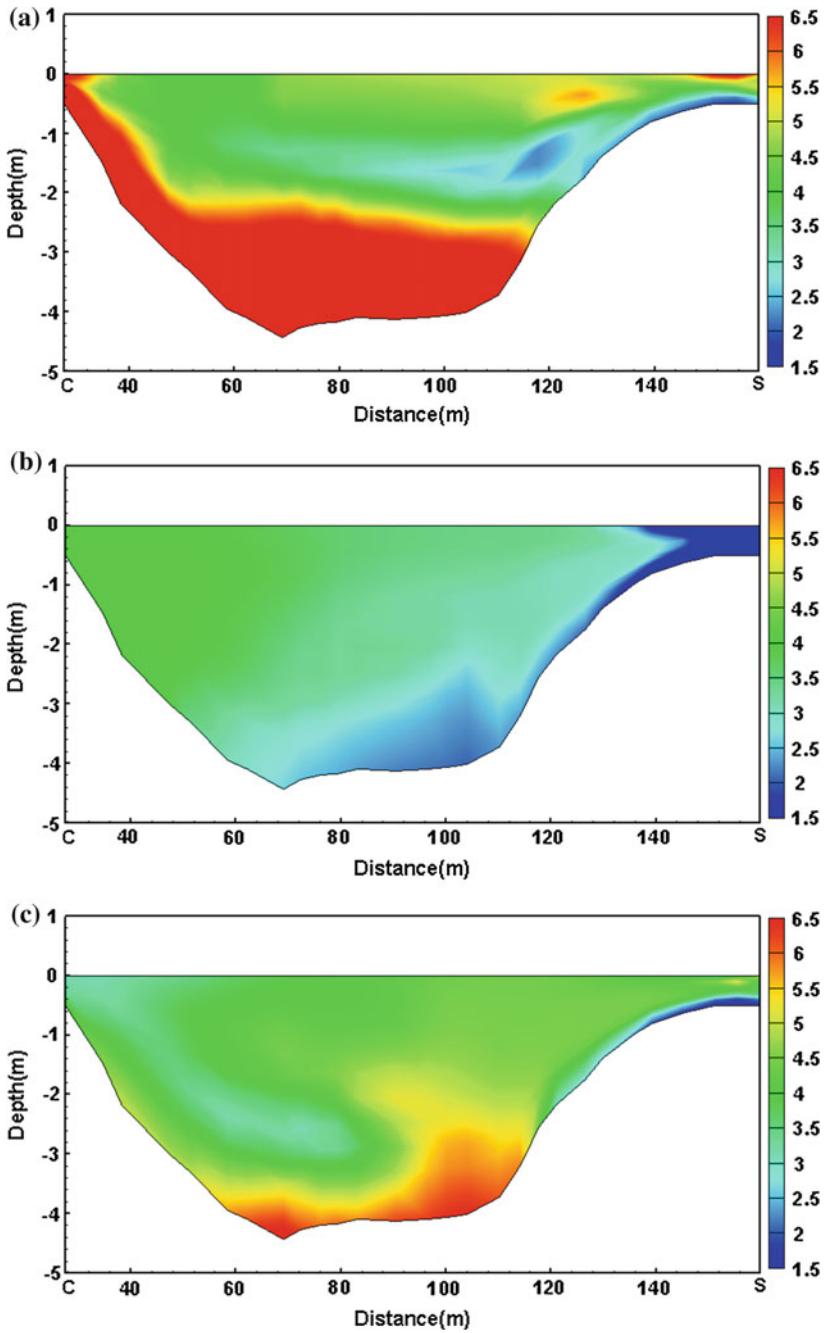


**Fig. 7** Tracer distribution at cross-section C–S under the 0.6 m<sup>3</sup>/s discharge condition at 48th h **a** without wind effect, **b** with northeast wind, and **c** with southwest wind

## 6 Conclusions

A three-dimensional hydrodynamic and hydrothermal model was implemented and applied to the subtropical alpine Yuan-Yang Lake (YYL) in the northeastern region of Taiwan. The model was verified with measured water surface elevation, current, and water temperature in 2008. Overall the model simulation results are in reasonable agreements with observations. Through the verification results, we also found that water temperature exhibited more mixing condition during the high rainfall event, while more stratification occurred during the normal condition.

The validated model was also used to calculate the mean residence time in response to different inflows with and without wind effects. Regression analysis of model results reveals that an exponential equation can be used to correlate the residence time to change of inflow discharges. The calculated system residence time is strongly dependent on the inflows and wind effects. The residence time decreases as the inflow discharge increases. The residence time without wind stress is higher than that with wind effect, indicating that wind plays an important role in lake mixing. The simulated results reveal that residence time is approximately 2–2.5 days under low inflow with wind effect. Because the residence time is an important indicator for lake water quality and ecosystem assessments, results from this study are helpful for environmental management of the YYL.

**Acknowledgments** This study was supported by the National Science Council and Academia Sinica, Taiwan, under the grant number NSC-96-2628-E-239-012-MY3 and AS-98-TP-B06, respectively. The financial support is highly appreciated.

## References

1. Branco, B. (2007). *Coupled physical and biogeochemical dynamics in shallow aquatic systems: Observation, theory and models*. The University of Connecticut, 223 p.
2. Branco, B., & Torgersen, T. (2009). Predicting the onset of thermal stratification in shallow inland waterbodies. *Aquatic Sciences*, 71(1), 65–79.
3. Cole, T. M., & Wells, S. A. (2000). *Hydrodynamic modeling with application to CE-QUAL-W2*. Portland, OR: Workshop Notes, Portland State University.
4. Edinger, J. E., & Buchak, E. M. (1983). *Development in LARM2: A longitudinal-vertical, time-varying, time-varying hydrodynamic reservoir model*. US Army Corps of Engineers Waterways Experiment Station Technical Report.
5. Falconer, R. A. (1986). Water quality simulation study of a natural harbor. *Journal of Waterway, Port, Coastal, and Ocean Engineering ASCE*, 112(1), 15–34.
6. Ford, P. W., Boon, P. I., & Lee, K. (2001). Methane and oxygen dynamics in a shallow floodplain lake: the significance of periodic stratification. *Hydrobiologia*, 485(1–3), 97–110.
7. Ganf, G. G. (1974). Diurnal mixing and the vertical distribution of phytoplankton in a shallow equatorial lake (Lake George, Uganda). *Journal of Ecology*, 62(2), 611–629.
8. Havens, K. E., Jin, K. R., Nenad, I., & Thomas, J. R. (2007). Phosphorus dynamics at multiple time scales in the pelagic zone of a large shallow lake in Florida, USA. *Hydrobiologia*, 581(1), 25–42.

9. Lap, B. Q., & Mori, K. (2007). A two-dimensional numerical model of wind-induced flow and water quality in closed water bodies. *Paddy and Water Environment*, 5(1), 29–40.
10. Liu, W.C., Chen, W.B., & Wu, C.H. (2008). Modelling effects of realignment of Keelung River, Taiwan. *Proceedings of the Institution of Civil Engineers-maritime Engineering*, 161(2), 73–87.
11. Kimura, N., Liu, W. C., Chiu, C. Y., Kratz, T. K., & Chen, W. B. (2012). Real-time observation and prediction of physical processes in a typhoon-affected lake. *Paddy and Water Environment*, 10(1), 17–30.
12. Persson, I., & Jones, I. D. (2008). The effect of water color on lake hydrodynamics: a modeling study. *Freshwater Biology*, 53(12), 2345–2355.
13. Rueda, F., Moreno-Ostos, E., & Armengol, J. (2006). The residence time of river water in reservoirs. *Ecological Modelling*, 191(2), 260–274.
14. Shchepetkin, A. F., & McWilliams, J. C. (2003). A method for computing horizontal pressure-gradient force in an oceanic model with a nonaligned vertical coordinate. *Journal Geophysical Research*, 108(C3), 3090.
15. Umlauf, L., & Buchard, H. (2003). A generic length-scale equation for geophysical turbulence models. *Journal of Marine Research*, 61(2), 235–265.
16. Yuan, H. L., & Wu, C. H. (2004). An implicit three-dimensional fully non-hydrostatic model for free-surface flows. *International Journal for Numerical Methods in Fluids*, 46(7), 709–733.
17. Zhang, Y. L., & Baptista, A. M. (2008). SELFE: A semi-implicit Eulerian-Lagrangian finite-element model for cross-scale ocean circulation. *Ocean Modelling*, 21(3–4), 71–96.